

Quantum Computation in a One-Dimensional Crystal Lattice with NMR Force Microscopy

T. D. Ladd, J. R. Goldman, A. Dâna, F. Yamaguchi, and Y. Yamamoto[†]

Quantum Entanglement Project, ICORP, JST

Edward L. Ginzton Laboratory, Stanford University, Stanford, California 94305-4085

(October 25, 2018)

A proposal for a scalable, solid-state implementation of a quantum computer is presented. Qubits are fluorine nuclear spins in a solid crystal of fluorapatite [$\text{Ca}_5\text{F}(\text{PO}_4)_3$] with resonant frequencies separated by a large field gradient. Quantum logic is accomplished using nuclear-nuclear dipolar couplings with decoupling and selective recoupling RF pulse sequences. Magnetic resonance force microscopy is used for readout. As many as 300 qubits can be implemented in the realistic laboratory extremes of $T = 10$ mK and $B_0 = 20$ T with the existing sensitivity of force microscopy.

PACS numbers: 03.67.Lx, 76.60.Pc, 07.79.Pk

An increasing number of theoretical developments have recently motivated the construction of a quantum computer with a large number of qubits. The potential for efficient simulation of quantum systems [1], the discoveries of algorithms for fast factorization [2] and database searching [3], and the development of quantum error correction [4] have helped to spur a large number of proposals for experimental implementations of a quantum computer. However, any physical implementation of a quantum computer must battle the fact that well-isolated quantum systems are difficult to couple and to measure, whereas the introduction of necessary couplings and probes leads to the devastating effects of decoherence.

To date, the most successful experimental realization of a multi-qubit quantum computer (or at least a simulation thereof) has been in room-temperature solution NMR [5]. Here, the spin-states of molecular nuclei in a solution are well isolated, as demonstrated by long thermal relaxation times (T_1) of many seconds. The nuclei of each molecule are weakly coupled by scalar couplings. Measurement without substantial decoherence is made possible by the large ensemble of $\sim 10^{22}$ uncoupled, identical molecules in the solution. There is much debate, however, as to whether solution NMR currently does or ever will exhibit the signatures of truly *quantum* information processing [6]. The presence of a large, mixed ensemble renders quantum entanglement and wave-function collapse of individual spins unmeasurable. Certain manipulations allow the processing of an “effective pure state” in which the ensemble behaves nearly identically to a single quantum system [5,7]. However, it has been shown that the evolution of effective pure states of existing solution NMR computers can be described without any entanglement, and either more qubits or much larger

nuclear polarizations will be needed before entanglement is demonstrable [8]. Even if we neglect the debate of what is “quantum” and what is not, the principal limitation due to the small polarizations in solution NMR quantum computation is that the usable signal decreases exponentially with the number of qubits, leaving this method unlikely to exceed the 10 qubit level without extensive modification [9].

In this letter, we propose an implementation using solid-state NMR. In a solid crystal there exists the potential for polarization of the nuclear spins by simple cooling of the lattice to extremely low temperatures. The thermal relaxation time T_1 can be dramatically lengthened when moving from a solution to an insulating, nonmagnetic crystal, and the nuclear-nuclear coupling can be faster. Hence, a solid crystal has great potential for quantum computation in terms of timescales [10] and scalability.

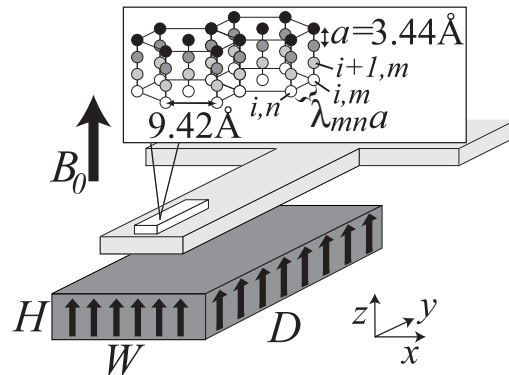


FIG. 1. The fluorapatite crystal, of length $10 \mu\text{m}$ and width roughly $1 \mu\text{m}$, is mounted near the end of a cantilever. A dysprosium micromagnet with dimensions $W = 10 \mu\text{m}$, $H = 4 \mu\text{m}$, $D = 400 \mu\text{m}$ is aligned parallel to the crystal planes. A field gradient of $1.4 \text{ T}/\mu\text{m}$ is produced at the crystal, a distance of $2.07 \mu\text{m}$ above the magnet. The insert shows the ^{19}F sites of the crystal structure. The different shades indicate different resonant frequencies.

These advantages, however, come at a cost: several difficult and related problems arise in implementing a solid-crystal NMR computer. This letter, although not the first proposal for quantum computation in a crystal lattice [11], provides new approaches to these problems. One problem is the complicated network of dipolar couplings in a solid, which must be suppressed to slow T_2

decoherence but selectively retained for logic. We address this problem with both “selective averaging” radio frequency (RF) pulse sequences and a well-chosen crystal structure. Another problem arises from the need to distinguish and detect nuclei in the periodic lattice of a crystal; for this we establish a very large, static, one-dimensional magnetic field gradient with a microfabricated, high-magnetization ferromagnet [12]. Only a small ensemble of nuclei may fit into the area over which the gradient field is homogeneous, and therefore a more sensitive means than standard inductive pick-up is needed to measure the nuclear spin states. We propose using magnetic resonance force microscopy (MRFM).

A schematic for the solid-crystal quantum computer we propose appears in Fig. 1. The quantum computer is an ensemble of N one-dimensional chains of n spin-1/2 nuclei. Due to the field gradient, the resonant frequencies of the nuclear spins within a chain are different. Hence the secular component of the dipolar Hamiltonian which couples the i th spin to the j th spin within the m th chain is written [13]

$$\begin{aligned}\hat{\mathcal{H}}_{ijmm} &= \frac{\mu_0}{4\pi}\gamma^2\hbar^2\frac{1-3\cos^2\phi}{[|j-i|a]^3}\hat{I}_{im}^z\hat{I}_{jm}^z \\ &\equiv \hbar\delta\omega_{ij}\hat{I}_{im}^z\hat{I}_{jm}^z,\end{aligned}\quad (1)$$

where γ is the gyromagnetic ratio ($2\pi \times 40$ MHz/T for ^{19}F), a is the distance between spins in a chain, and ϕ is the angle between the chain of spins and the large applied magnetic field, which is taken to be in the z -direction. Other terms of the dipolar Hamiltonian average to zero on a timescale of $1/\Delta\omega_{ij}$ or faster, where $\Delta\omega_{ij} = \gamma a|\nabla B_{ij}^z|$ is the separation of the i th and j th resonant frequencies caused by the field gradient ∇B_{ij}^z between them. The Hamiltonian of Eq. (1) may be “switched off” by applying a periodic succession of narrow band π pulses at, for instance, the i th resonant frequency [13]. Simultaneous decoupling of more than two qubits may be accomplished by timing the selective π pulses according to the entries of an appropriately sized Hadamard matrix; a pair of qubits may be selectively recoupled in order to implement two-bit gates [14].

Non-disturbing measurement is possible in this scheme because, orthogonal to the chain direction, a nucleus of resonant frequency ω_i has a large plane of copies with equal frequency. The coupling between copies has a different form; the n th and m th nucleus of identical resonant frequency ω_i are coupled by the Hamiltonian [13]

$$\hat{\mathcal{H}}_{iimn} = \frac{1}{2}\frac{\mu_0}{4\pi}\gamma^2\hbar^2\frac{1-3\cos^2\theta_{mn}}{(a\lambda_{mn})^3}\left(3\hat{I}_{im}^z\hat{I}_{in}^z - \hat{\mathbf{I}}_{im} \cdot \hat{\mathbf{I}}_{in}\right),$$

where λ_{mn} is the distance between the two nuclei in units of a , and θ_{mn} is the angle between the vector which connects them and the direction of the applied field. This coupling between copies must be “switched off” to prevent interference between ensemble members. Decoupling these spins may be done by any number of pulse

sequences which have been developed over the past 40 years in solid-state NMR, the simplest of which is the WAHUHA pulse sequence. Such sequences can reduce dipolar broadening by more than three orders of magnitude [15].

Fortunately, the different forms of $\hat{\mathcal{H}}_{ijmm}$ and $\hat{\mathcal{H}}_{iimn}$ allow constant decoupling of copies without adverse effect on the manipulations of couplings within individual computers. The qubit-qubit coupling of Eq. (1) may in general be rescaled and rotated by the broadband WAHUHA-type sequence, but it may still be controlled for logic gates with suitably phased π pulses. The broadband WAHUHA-type pulse sequence which decouples all copies is unaffected by the addition of selective π -pulses, insofar as those π -pulses are sufficiently short in comparison to the pulse spacing. This criterion is difficult to meet, since the π pulses must last a time of about $1/\Delta\omega_{i,i+1}$ to be frequency selective. A simple example to illustrate the decoupling scheme is shown in Fig. 2. This example is limited by the adverse effect of the finite π pulse-length on the WAHUHA decoupling, but longer and more sophisticated sequences can be designed with standard techniques to compensate for this and other limiting effects [15].

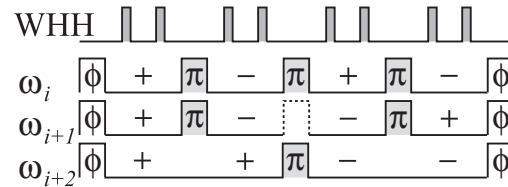


FIG. 2. An example RF pulse sequence. The first line (WHH) shows broadband decoupling of qubit copies; the narrow, shaded pulses are appropriately phased $\pi/2$ pulses [15], made sufficiently narrow (broadband) to affect all nuclei in the crystal. The subsequent three lines show selective pulses to decouple qubits; these wider pulses are sufficiently long (narrowband) to affect only individual planes. Single spin rotations, denoted by ϕ , may be performed in between cycles. Multi-bit gates such as controlled-NOT may be performed by combining single spin rotations with selective recoupling. For example, qubits i and $i+1$ may be recoupled by adding a π pulse at the time noted by the dotted line [14].

The only problematic dipolar couplings which remain after applying the pulse sequences described above are those between qubits with different resonant frequencies ($i \neq j$) and in different chains ($m \neq n$). These couplings only arise when two planes of qubits are selectively recoupled during a two-bit gate. The needed time duration for a logic operation may be minimized by maximizing the desired qubit-qubit coupling – this is accomplished by first letting a be the smallest nuclear distance in the crystal. Second, we set $\phi = 0$, hence putting the gradient parallel to the applied field. Third, only nearest-neighbor qubit couplings are used ($j = i+1$), with longer distance

couplings accomplished by bit-swapping [16]. After making these choices, we have $\delta\omega \equiv \delta\omega_{i,i+1} = -\mu_0\gamma^2\hbar/2\pi a^3$, and the target qubit of frequency ω_i in the m th chain is coupled to control qubit copies at ω_{i+1} in the other chains by the Hamiltonian

$$\begin{aligned}\hat{\mathcal{H}}_{im}^* &= -\hbar\delta\omega \sum_n \frac{\lambda_{mn}^2 - 2}{2(1 + \lambda_{mn}^2)^{5/2}} \hat{I}_{im}^z \hat{I}_{i+1,n}^z \\ &\equiv -\hbar\delta\omega \sum_n b_{mn} \hat{I}_{im}^z \hat{I}_{i+1,n}^z.\end{aligned}\quad (2)$$

The decoherence caused by this undesired Hamiltonian is minimized if the coupling constants are sufficiently small to obey

$$\frac{\sigma}{\delta\omega} = \frac{1}{2} \sqrt{\sum_n b_{mn}^2} \ll 1, \quad (3)$$

where σ (the square root of the second moment [15]) is the effective linewidth of the qubit ensemble during recoupling, which we demand to be much smaller than the splitting $\delta\omega$. This inequality is best satisfied by a crystal whose nuclei couple only in isolated chains.

A crystal which approximates this description is fluorapatite, $\text{Ca}_5\text{F}(\text{PO}_4)_3$, whose ^{19}F structure is shown in Fig. 1. In fluorapatite, we find $\sigma/\delta\omega \approx 1/58$, roughly six times smaller than in a simple cubic crystal such as CaF_2 . The one-dimensional nuclear structure of fluorapatite has been recognized in several NMR experiments [17]. Decoherence timescales in this crystal are analogous to the well-known case of CaF_2 . The T_2 time is limited by dipolar broadening; if dipolar couplings are perfectly controlled, the timescale for internal decoherence is pushed toward the spin-lattice relaxation time constant T_1 , which is limited by thermal fluctuations of paramagnetic impurities (rare-earth substitutions, for example) and can easily be several hours for reasonable crystal purities and temperatures [18].

The field gradient is accomplished by a micron-sized ferromagnetic parallelepiped. Calculations similar to those in Ref. [12] show that such a magnet, made of dysprosium and placed in a 7 T external field as shown in Fig. 1, can produce a field gradient of 1.4 T/ μm at a distance of 2.07 μm above the magnet, which leads to $\Delta\omega \equiv \Delta\omega_{i,i+1} = 2\pi \times 19.2$ kHz. A 1 μm by 10 μm fluorapatite crystal above the magnet contains $N = 10^7$ equivalent-frequency qubit copies in each xy -plane. The field variation along the y -direction is negligible since the magnet is much longer than the crystal. The field variation along the x -axis is sufficiently small that all of the equivalent-frequency nuclei lie within a bandwidth of $\Delta\omega$. We also note that inhomogeneous broadening is constantly refocused in this scheme by the narrow-band π pulse sequences during both decoupling and selective recoupling.

The presence of a large magnetic field gradient provides a natural means for performing MRFM on a magnetization M^z , since this technique is sensitive to the gradient

force given by $F = M^z \nabla B^z$ [19]. The crystal is mounted on a microfabricated cantilever which oscillates in the z -direction, as in Fig. 1. The long axis of the crystal-cantilever heterostructure and magnet are aligned. The experiment is performed in high vacuum ($< 10^{-5}$ torr) and at low temperatures. A coil is used to generate the RF pulses for logic operations and decoupling sequences; it also generates the continuous-wave radiation for readout. An optical fiber-based displacement sensor is used to monitor deflection of the cantilever using interferometry. Sub-Ångstrom oscillations can be detected; larger oscillations can be damped with active feedback which avoids additional broadening while maintaining high sensitivity [20,21].

Readout is performed using cyclic adiabatic inversion [22], which modulates the magnetization of a plane of nuclei at a frequency near or on resonance with the cantilever. The spins of resonant frequency ω_i are irradiated with the RF field $B^x = 2B_1 \cos\{\omega_i t - (\Omega/\omega_m) \cos(\omega_m t)\}$, where ω_m is the modulation frequency chosen to be near the resonance of the cantilever, and Ω is the frequency excursion, which should be much smaller than $\Delta\omega$ [23]. Simultaneous detection of signal from multiple planes is possible if the different planes to be measured are driven at distinct modulation frequencies ω_m .

The force resolution for MRFM is limited by thermal fluctuations of the cantilever [24]. Force resolutions of 5.6×10^{-18} N/ $\sqrt{\text{Hz}}$ have been reported for single crystal cantilevers at 4 K [25]. To estimate the force involved in a measurement following a quantum computation, we consider the case in which initialization is imperfect, so that the temperature T is non-zero and an effective pure state must be used [5,7]. The usable magnetization is estimated [9] as

$$M^z = \gamma\hbar \frac{N \sinh(n\hbar\gamma B_0/2k_B T)}{2^n \cosh^n(\hbar\gamma B_0/2k_B T)}.$$

In the high temperature limit, this magnetization approximates to $(\gamma^2\hbar^2 B_0/2k_B T) N n 2^{-n}$ showing the exponential downscaling which plagues solution NMR. Even in this limit, with the relatively small N of 10^7 and using the field gradient described above in a 7 T field at 4 K, the force which needs to be measured works out to about $10^{-15} n 2^{-n}$ newtons, allowing $n \sim 10$ qubits. The density matrix of such a system would be outside the neighborhood in which it has been shown that all density matrices are separable [8]. As seen in Fig. 3, the situation is improved in larger fields and at lower temperatures, where M^z improves exponentially in B_0/T . In the realistic laboratory extreme $B_0 = 20$ T and $T = 10$ mK, this design may scale to $n \sim 300$ qubits; in this regime entanglement is shown to be demonstrable [8].

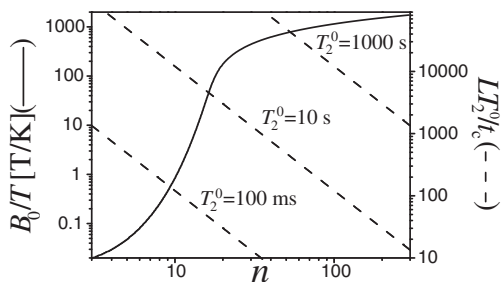


FIG. 3. A plot showing the scalability of the present scheme. The solid curve, corresponding to the left axis, shows the magnetic field (in T) divided by temperature (in K) needed in order for a number of qubits n to be measurable. The dashed lines, corresponding to the right axis, plot the number of logic gates (decoherence time T_2^0 divided by the pulse sequence cycle time t_c) times the length of a “block” of the decoupling sequence L against n for several values of T_2^0 .

A primary limitation to the long-term scalability of this scheme is the number of logic gates which can fit into the decoherence time when there is a large number of qubits. The decoupling/recoupling pulse scheme based on Hadamard matrices has a cycle time $t_c(n)$ of $Ln^2/\Delta\omega$, where the parameter L depends on the length of the homonuclear decoupling subsequence and only weakly on the number of qubits n [14]. Since single spin rotations must occur between cycles, the clock speed is set by this cycle time. The number of logic gates we may perform is approximately $t_c(n)$ divided into the remaining decoherence time T_2^0 . This timescale T_2^0 is due to residual homonuclear couplings, cantilever thermal drift, and thermal relaxation resulting from magnetic impurities; these contributions are limited by the experimental performance of the homonuclear decoupling pulse sequence, cantilever feedback stabilization, and crystal growth technique, respectively. Figure 3 shows the number of logic gates possible for several values of T_2^0 . The bottom dashed trace ($T_2^0 = 100$ ms) corresponds to the case in which homonuclear couplings are perfectly controlled but cantilever drift is completely unsuppressed, while the middle ($T_2^0 = 10$ s) and top ($T_2^0 = 1000$ s) traces assume suppression by 20 and 40 dB with a negative feedback circuit. The limited number of gates at high numbers of qubits is a remaining problem which may be addressed through error correcting codes [4], more sophisticated pulse sequences, or the use of a more one-dimensional system [26].

A remaining challenge in this scheme is the alignment of the field gradient, cantilever, and crystal. Such alignment is critical, and although difficult, it is not impossible with modern microfabrication technology and feedback control using micro-electro-mechanical actuators [27].

This proposal features two important advantages over schemes using solid-state NMR with impurity dopants [28]. The fabrication difficulty of artificially implanting controlled arrays of spins is avoided in our proposal by

using nuclei that are naturally organized into a crystal structure. Also, the use of an ensemble of 10^7 spins avoids the need for the daunting task of reading and initializing single nuclear spins. Indeed, ensemble measurement has given solution NMR a developmental head-start against other existing proposals for quantum computation, and it is hoped that the scheme presented here will carry NMR quantum computation onward to the many-qubit regime.

This work was partially supported by NTT Basic Research Laboratories. T. D. L. was supported by the Fannie and John Hertz Foundation.

[†] Also at NTT Basic Research Laboratories, 3-1 Morinosato-Wakamiya Atsugi, Kanagawa, 243-0198, Japan.

- [1] R. P. Feynman, *Int. J. Theor. Phys.* **21**, 467 (1982); S. Lloyd, *Science* **273**, 1073 (1996).
- [2] P. W. Shor, in *Proceedings of the 35th Symposium on the Foundations of Computer Science* (IEEE Computer Society Press, Los Alamitos, 1994), p. 124.
- [3] L. K. Grover, *Phys. Rev. Lett.* **79**, 325 (1997).
- [4] P. W. Shor, *Phys. Rev. A* **52**, R2493 (1995).
- [5] N. A. Gershenfeld and I. Chuang, *Science* **275**, 350 (1997); D. G. Cory, A. F. Fahmy, and T. F. Havel, *Proc. Natl. Acad. Sci. USA* **94**, 1634 (1997).
- [6] R. Schack and C. M. Caves, *Phys. Rev. A* **60**, 4354 (1999).
- [7] E. Knill, I. Chuang, and R. Laflamme, *Phys. Rev. A* **57**, 3348 (1998).
- [8] S. L. Braunstein *et al.*, *Phys. Rev. Lett.* **83**, 1054 (1999).
- [9] W. S. Warren, *Science* **277**, 1688 (1997).
- [10] T. D. Ladd, J. R. Goldman, F. Yamaguchi, and Y. Yamamoto, *Appl. Phys. A* **71**, 27 (2000).
- [11] F. Yamaguchi and Y. Yamamoto, *Appl. Phys. A* **68**, 1 (1999).
- [12] J. R. Goldman, T. D. Ladd, F. Yamaguchi, and Y. Yamamoto, *Appl. Phys. A* **71**, 11 (2000).
- [13] C. P. Slichter, *Principles of Magnetic Resonance* 3rd Ed. (Springer, Berlin, 1990).
- [14] D. W. Leung, I. L. Chuang, F. Yamaguchi, and Y. Yamamoto, *Phys. Rev. A* **61**, 042310 (1999).
- [15] U. Haeberlin, *High Resolution NMR in Solids: Selective Averaging* (Academic Press, New York, 1976); M. Mehring, *High Resolution NMR in Solids* (Springer-Verlag, Berlin, 1983).
- [16] S. Lloyd, *Science* **261**, 1569 (1993).
- [17] W. Van Der Lugt and W. J. Caspers, *Physica* **30**, 1658 (1964); M. Engelsberg, I. J. Lowe, and J. L. Carolan, *Phys. Rev. B* **7**, 924 (1973); G. Cho and J. P. Yesinowski, *J. Phys. Chem.* **100**, 15716 (1996).
- [18] N. Bloembergen, *Physica* **15**, 386 (1949).
- [19] J. A. Sidles, *Appl. Phys. Lett.* **58**, 2854 (1991); D. Rugar, C. S. Yannoni, and J. A. Sidles, *Nature* **360**, 563 (1992).
- [20] U. Dürig, H. R. Steinauer, and N. Blanc, *J. Appl. Phys.* **8**, 3641 (1997).

- [21] A calculation using Redfield theory [13] with the thermal noise statistics of a high-sensitivity cantilever [24] estimates the T_2 timescale due to the cantilever's thermal drift as $T_2 = k\omega_c Q a^2 / \Delta\omega^2 k_B T \approx 200$ ms, where $k \approx 10^{-3}$ N/m is the spring constant, $\omega_c/2\pi \approx 10$ kHz is the resonant frequency, and $Q \approx 20,000$ is the quality factor of the cantilever. Active feedback stabilization is expected to increase this timescale by as many as four orders of magnitude, bringing it close to the lengthy T_1 timescale.
- [22] A. Abragam, Principles of Nuclear Magnetism (Oxford University Press, 1961).
- [23] D. Rugar *et al.*, Science **264**, 1560 (1994).
- [24] T. B. Gabrielson, IEEE Trans. Electron Devices **40:5**, 903 (1993).
- [25] T. D. Stowe *et al.*, Appl. Phys. Lett. **71**, 288 (1997).
- [26] In a perfectly one-dimensional system with high n , the Hadamard decoupling scheme may be truncated to decouple sets of only $n_d < n$ nearest neighbors and then repeated periodically along a chain. The remaining couplings result in decoherence with a timescale T_2^{qd} which scales as n_d^3 , and since $t_c \sim n_d^2$, T_2/t_c may be made arbitrarily large with large enough T_2^0 . (In the real crystal fluorapatite, once $n_d > \lambda_{m,m+1} = 2.74$, the contributions of the ensemble of copy-nuclei causes $T_2^{\text{qd}} \sim n_d^2$, leading to a constant T_2^{qd}/t_c which is too small to be useful.)
- [27] S. A. Miller, K. L. Turner, and N. C. MacDonald, Rev. Sci. Instrum. **68**, 4155 (1997).
- [28] B. E. Kane, Nature **393**, 133 (1998); G.P. Berman, G. D. Doolen, P. C. Hammel, and V. I. Tsifrinovich, Phys. Rev. B **61**, 14694 (2000).